II. MICROWAVE GASEOUS DISCHARGES*

Prof. S. C. Brown
Prof. W. P. Allis
Prof. D. C. White
Prof. R. C. Booton
Dr. D. O. Akhurst
Dr. G. Bekefi
Dr. S. J. Buchsbaum
Dr. E. I. Gordon
Dr. M. P. Madan
H. Fields
J. L. Hirshfield
W. R. Kittredge
J. J. McCarthy
R. G. Meyerand, Jr.
W. J. Mulligan
D. R. Whitehouse

A. HIGHLY IONIZED PLASMAS

The study of methods for the production of highly ionized plasmas by using a conventional 50-watt cw magnetron continues. The interaction of a high-density plasma in a magnetic field with a microwave field is still not well understood. The systematic study of this interaction is complicated by the presence of plasma oscillations in our discharge. The oscillations are in the megacycle region (indicating that they may result from collective ion motion) and depend strongly on the magnetic field. The presence of oscillations can be detected either by the microwave circuit or by monitoring the light output of the discharge. The microwave method is the more sensitive of the two, but whenever oscillations can be detected on the light output the oscillation frequency, as measured by both methods, is the same. The light modulation is approximately 5 per cent. The correlation between the plasma oscillation and the observed high-density plasma instabilities is being studied.

S. J. Buchsbaum, E. I. Gordon

B. EXPERIMENTAL DETERMINATION OF THE FREQUENCY OF ELECTRON LOSS IN A MICROWAVE-MAINTAINED PLASMA

The frequency of loss of electrons from a microwave-maintained hydrogen plasma situated in a uniform magnetic field was studied experimentally in the region of electron cyclotron resonance. The results show the dependence of the frequency of electron loss on the energy of the electrons and on the dimensions of the container.

The energy of an electron, moving under the influence of an alternating electric field, $E = E_o \cos \omega t$, perpendicular to a constant magnetic field B, can be shown to be

$$u_\perp = \frac{e^2 E_o^2 \sin^2\left[\frac{1}{2}(\omega - \omega_b)t\right]}{2m(\omega - \omega_b)^2} \qquad (1)$$

where ω_b is the electron cyclotron frequency. The initial velocity of the electrons is assumed to be zero. The dependence of the mean perpendicular energy on the strength

*This work was supported in part by the Atomic Energy Commission under Contract AT(30-1) 1842.

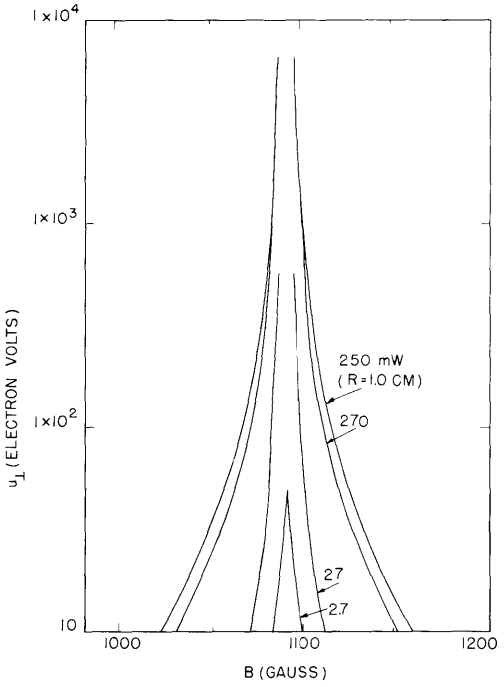

Fig. II-1. Electron energy perpendicular to the magnetic field as a function of the magnetic-field strength in the vicinity of electron cyclotron resonance.

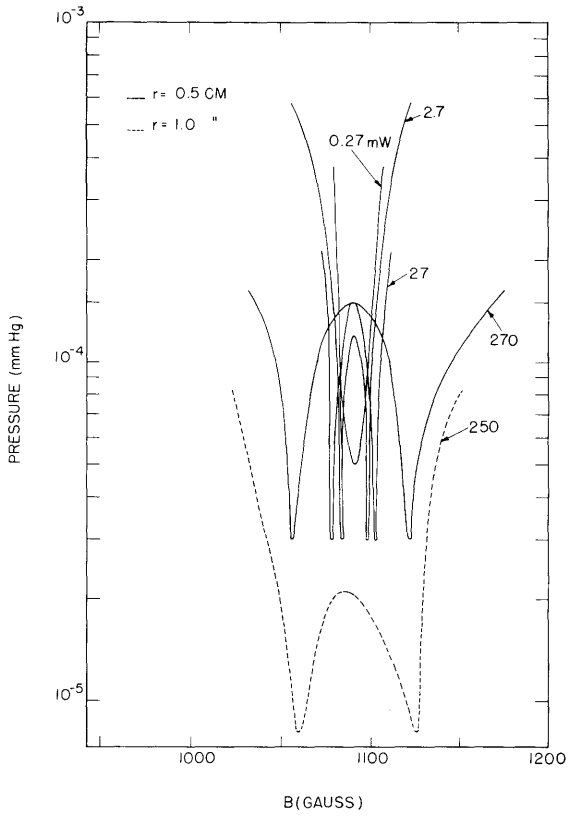

Fig. II-2. Limiting conditions of plasma maintenance as a function of magnetic-field strength in the vicinity of electron cyclotron resonance.

of the magnetic field in the vicinity of electron cyclotron resonance, as calculated from Eq. 1, is shown in Fig. II-1 for several values of incident power. The high energies to which electrons may be accelerated in the region of cyclotron resonance are several orders greater than energies off resonance.

Experimental results of the dependence of the microwave maintaining conditions on the value of the hydrogen gas pressure and the strength of the magnetic field are shown in Fig. II-2. These results were obtained by the experimental procedure outlined in the Quarterly Progress Report of January 15, 1957, page 17. In the experiments carried out with an incident microwave power of 250 mw, the gas was contained within a quartz tube of 1.0-cm internal radius; the results for other microwave powers were obtained with a tube of 0.5-cm internal radius. A comparison of the curves for microwave powers of 250 mw and 270 mw shows the effect of increasing the tube radius by a factor of two, the curve for the larger tube being displaced from the curve for the smaller tube by an order of magnitude in pressure. In the vicinity of cyclotron resonance, the

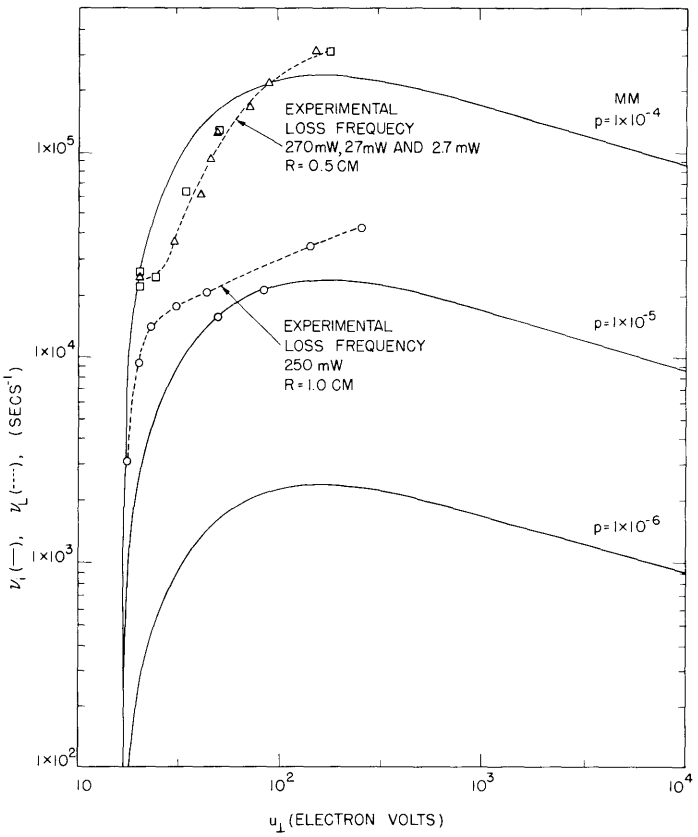

Fig. II-3. Electron ionization frequency for hydrogen and the constructed frequency of electron loss (for quartz tubes of 0.5-cm and 1.0-cm internal radii) as functions of electron energy.

conditions for maintaining the plasma coincide for the higher powers, indicating that the electron energy in the system may be limited. For microwave powers of 2.7 mw, 27 mw and 270 mw incident on the cavity, the minimum pressure for plasma maintenance is the same, the minima occurring at magnetic-field strengths displaced by nearly equal values from the magnetic field at cyclotron resonance.

For a given point on the curves of Fig. II-1, the corresponding value of electron energy can be determined from Fig. II-2. The electron energy and the gas pressure determine the rate at which electrons are produced by ionization, as shown in Fig. II-3. In equilibrium the rate at which electrons are lost is equal to the rate at which they are produced by ionization, consequently the loss frequency associated with each point on Fig. II-1 can be determined. The electron-loss frequency as a function of energy is shown in Fig. II-3.

The results indicate that the frequency of electron loss for the quartz tube of 0.5-cm internal radius is greater than the frequency of electron loss for the quartz tube of 1.0-cm internal radius by a factor of 3.5 to 8.0, depending on the electron energy.

D. O. Akhurst

C. HIGH-FREQUENCY BREAKDOWN IN MAGNETIC FIELDS

To further our understanding of the loss mechanisms in microwave discharges with magnetic fields, breakdown data for hydrogen were obtained in a TM_{010}-mode cylindrical cavity with a uniform static magnetic field at right angles to the electric field in the cavity. The cavity of OFHC copper (radius, 3.5 cm; height, 0.34 cm) had an unloaded Q of 1550. It could be evacuated after bake-out to pressures better than 10^{-8} mm Hg before admitting hydrogen from the decomposition of uranium hydride. In this experiment the pressure range extended three orders of magnitude below the published helium data of Lax, Allis, and Brown (1). Breakdown was observed either by noting a jump in the standing-wave minimum as the discharge came on and altered the cavity-coupling coefficient, or by observing with a phototube the onset of light from the discharge. The magnetic-field changes were measured with a deflection potentiometer that is accurate to four places.

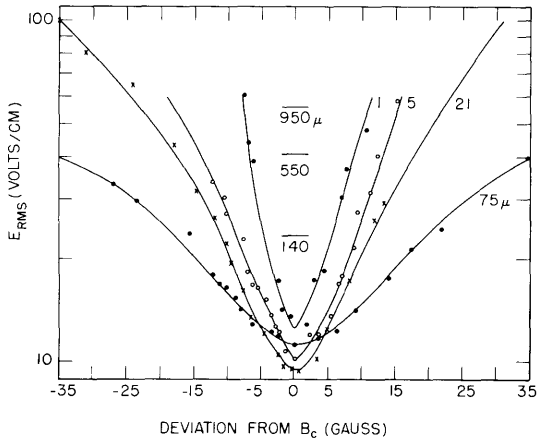

Fig. II-4. Breakdown field strengths in hydrogen as a function of magnetic field for various gas pressures.

Figure II-4 shows the breakdown field strengths as a function of magnetic field for several low-pressure runs. Minima for three higher pressure curves, which would be quite broad on this scale, are also indicated. Figure II-5 is a plot of the minimum breakdown field strengths as a function of pressure.

The effective electric field near resonance (1) can be shown to be proportional to $\left[(\omega - \omega_b)^2 + \nu_c^2\right]^{-1/2}$, where $\omega_b = eB/m$ is the cyclotron radian frequency corresponding to the magnetic field B, ω is the microwave radian frequency, and ν_c is the collision frequency. Thus the breakdown curves should rise to $\sqrt{2}$ times their minimum value when $\omega - \omega_b = \nu_c$ in order to maintain a constant effective electric field. These half-power widths are shown as points in Fig. II-6. For comparison, the approximate value of ν_c in hydrogen (2) is also shown. As we would expect, sharp deviations between these two quantities set in when diffusion is no longer the governing loss mechanism, i.e., below the pressure at which the mean free path is longer than the tube dimensions. The mean free path, computed on the assumption of a Maxwellian distribution for the electrons, is $\ell = 1/\nu_c\ (8kT/\pi m)^{1/2}$. For an average electron energy of 3 ev and diffusion assumed along the magnetic field only, the mean free path equals the diffusion length at a pressure of 14.7 μ Hg. This

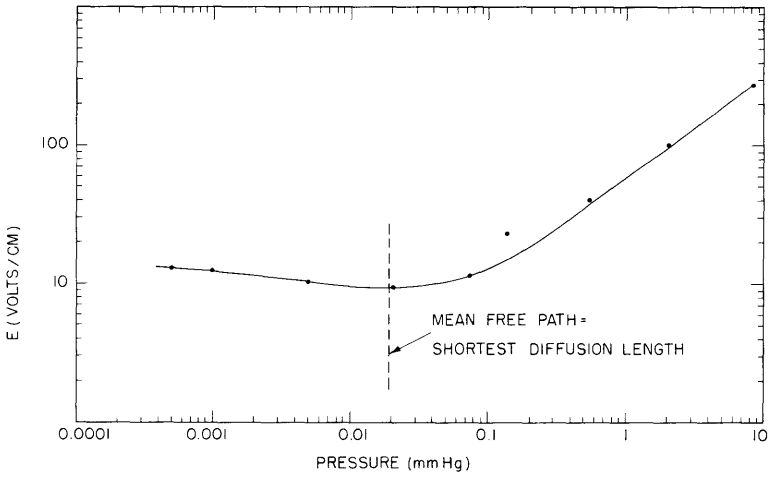

Fig. II-5. Minimum breakdown field strength as a function of gas pressure.

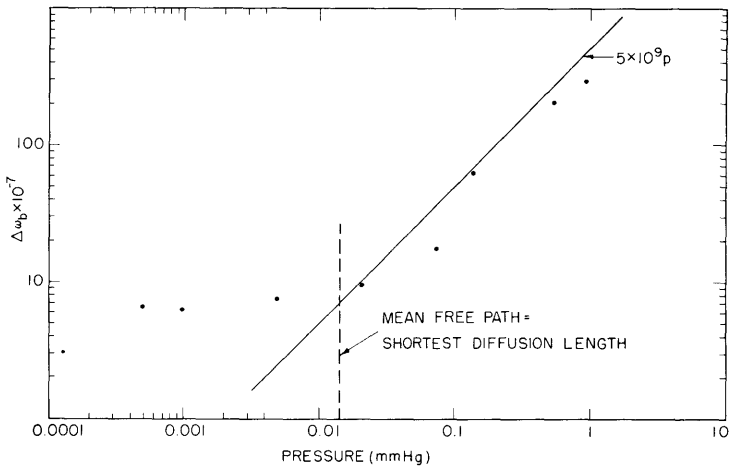

Fig. II-6. Half-power widths of breakdown curves as a function of pressure.

is shown as a dotted vertical line in Figs. II-2 and II-3.

We plan to extend these measurements to lower pressures, as well as to repeat them with quartz walls, in the hope of constructing a suitable low-pressure, loss-mechanism theory in these discharges.

J. L. Hirshfield, H. Fields

References

1. B. Lax, W. P. Allis, and S. C. Brown, J. Appl. Phys. 21, 1297-1304 (1950).
2. S. C. Brown and W. P. Allis, Basic data of electrical discharges, Third Edition, Technical Report 283, Research Laboratory of Electronics, M.I.T., Sept. 1, 1956.

D. MICROWAVE DETERMINATION OF PLASMA DENSITY DISTRIBUTION

Conventional microwave methods cannot be used to determine plasma electron density at a point, but can be used to obtain an average density defined by

$$\langle n \rangle = \frac{\int n E^2 \, dv}{\int E^2 \, dv} = \alpha n_o \tag{1}$$

where E is the probing microwave electric field, and n_o is the central electron density in the cavity. The coefficient α is known if the electron density distribution is known. In many experiments, especially in those performed in the afterglow, the electron density distribution is not only unknown but also changes with time. In such experiments it is of importance to determine, directly if possible, the dependence of α on time.

This can be accomplished if the plasma is measured with two modes whose electric fields have different functional dependences in the plasma region. As an example, consider the TE_{011} and TE_{111} modes in a cylindrical cavity. The plasma is in the shape of a cylindrical post along the axis of the cavity. When the radius of the plasma is small compared with the radius of the cavity, then, over the radius of the plasma, the magnitude of the E field of the TE_{011} mode is proportional to the radius, and the field of the TE_{111} mode is independent of the radius. The z-dependence of the two modes is the same. If we assume that the dependence of plasma density on radius can be approximated by the function

$$n = n_o (1 - r^2/R^2)^\gamma \tag{2}$$

where R is the radius of the plasma post, then the ratio of the resonant-frequency shifts of the two modes that result from the plasma is

$$\frac{\Delta\omega_{TE_{011}}}{\Delta\omega_{TE_{111}}} = g \frac{\int_0^R (1 - r^2/R^2)^\gamma \, r^3 \, dr}{R^2 \int_0^R (1 - r^2/R^2)^\gamma \, r \, dr} = \frac{g}{\gamma + 2} \tag{3}$$

where g is a geometrical constant that does not depend on the density distribution. Hence, from a measurement of $\Delta\omega_{TE_{011}} / \Delta\omega_{TE_{111}}$, γ can be computed, and from it the approximate shape of the plasma density can be computed. When γ is small, the ratio of the frequency shifts is sensitive to small changes in γ. For example, the ratio changes more than 30 per cent when γ changes from zero (uniform plasma) to unity (which, to a good approximation, gives the actual density distribution in a cylindrical tube).

The ratio of the frequency shifts can be made even more dependent on γ if the two modes are so chosen that, over the plasma region, the field of one mode decreases with radius while the field of the other increases with radius. However, this requires the use of higher modes. Similarly, the dependence of the plasma density on the z-coordinate can be obtained approximately if two modes are utilized whose E-fields are different functions of z but have the same dependence on the radius in the plasma region. Two such modes are, for example, the TM_{010} and the TE_{111} modes.

S. J. Buchsbaum

E. PLASMA DIAMAGNETISM

Theoretical discussions of the diamagnetic effect of a cloud of relatively free electrons in a magnetic field have been carried on for more than forty years but little experimental work has been directed toward observing it (1). This diamagnetism, if it exists, is very small. We shall show that it is observable in high-density, high-temperature plasmas. Thus, diamagnetism could become useful as a diagnostic tool in plasmas for which the conventional methods that use probes or microwaves are unreliable. Probe theory is not adequate when magnetic fields are present, and microwave conductivity measurements are unreliable when the plasma frequency is close to the microwave frequency. Our experiment, which we hope will establish that the diamagnetic effect is observable and determine its validity as a diagnostic tool, is in the preliminary stage.

It is well known that a plasma in thermal equilibrium has no diamagnetic effect (2). In the following discussion we consider a plasma that is not in thermal equilibrium. It is an active plasma, in which ionizations occur throughout its volume and recombination with positive ions occurs at the walls of the container. It may also be a plasma in which ionization does not occur, so that the density of charged particles decays with time. In either case the controlling loss mechanism is assumed to be diffusion. We consider that a uniform magnetic field of magnitude B_o is present in the absence of the plasma. The geometry is cylindrical, and the tube containing the plasma is nonconducting and coaxial with the field.

We assume that there is only one species of ion, singly charged, in addition to the electrons. The flow of electrons or ions is given by

$$\vec{\Gamma}_{\pm} = -\overleftrightarrow{D}_{\pm} \cdot \operatorname{grad} n_{\pm} \pm \overleftrightarrow{\mu}_{\pm} \cdot \vec{E}_s n_{\pm} \tag{1}$$

in which $\overleftrightarrow{D}_{\pm}$ and $\overleftrightarrow{\mu}_{\pm}$ are the diffusion and mobility tensors for ions and electrons given by

$$\frac{\overleftrightarrow{D}}{D} = \frac{\overleftrightarrow{\mu}}{\mu} = \begin{Vmatrix} a & -b & 0 \\ b & a & 0 \\ 0 & 0 & 1 \end{Vmatrix} \tag{2}$$

in which D is the diffusion coefficient, and μ is the mobility in the absence of the magnetic field (3). For simplicity, D and μ are assumed constant, and are given by $D = 1/3 \langle v^2 \rangle / \nu_c$ and $\mu = e/m\ \nu_c$, where ν_c is the collision frequency with neutral or charged particles. The quantities a and b are given by $a = \nu_c^2 / \left(\nu_c^2 + \omega_b^2\right)$, $b = a\omega_b/\nu_c$, where $\omega_b = eB/m$ is positive for electrons and negative for ions. The density is denoted by n_+ and n_-. The space-charge field is denoted by E_s. The continuity equation for electrons and ions leads to

$$\operatorname{div} \vec{\Gamma}_+ = \operatorname{div} \vec{\Gamma}_- = \nu n_- \tag{3}$$

in which ν is either the rate of ionization in the steady state or the rate of decay or build-up in a changing plasma. From Eq. 3 we can write

$$e\left(\vec{\Gamma}_+ - \vec{\Gamma}_-\right) = \operatorname{curl} \vec{H} \tag{4}$$

Since the boundary conditions for an insulating container require that the r and z components of the current be zero, we assume that they are zero in the volume of the plasma. We assume that there is symmetry in the θ-direction, and hence that there is no azimuthal space-charge field. We also assume that we are in the limit of large densities where $\operatorname{grad} n_+/n_+ \approx \operatorname{grad} n_-/n_-$.

Equations 1 and 3 lead to the usual solution for diffusion in a magnetic field. There are currents of ions and electrons in the azimuthal direction which produce a longitudinal magnetic field opposite the applied field. It can be shown that

$$\left(\vec{\Gamma}_+ - \vec{\Gamma}_-\right)_\theta = \frac{\partial n_-}{\partial r}\, k\, \frac{(T_+ + T_-)}{e}\, \frac{\mu_-\mu_+ B}{1 + \mu_-\mu_+ B^2} \tag{5}$$

in which T_+ and T_- are the ion and electron temperatures, and k is Boltzmann's constant. Equation 5 is a good approximation, within the limits of the original assumptions, for densities above 10^8/cc, for almost any tube of reasonable size. The field at the wall of the tube is B_o, and the density is zero. If we write

$$e\left(\vec{\Gamma}_+ - \vec{\Gamma}_-\right)_\theta = -\frac{1}{\mu_o}\frac{\partial B}{\partial r} \tag{6}$$

and integrate, we obtain

$$\frac{\ln B/B_o}{\mu_+\mu_-} + \frac{1}{2}\left(B^2 - B_o^2\right) = -\mu_o\, k(T_+ + T_-)n \tag{7}$$

If we write $B = B_o + \delta B$, $\delta B \ll B_o$, we obtain

$$\delta B = - \frac{\mu_+ \mu_- B_o^2}{1 + \mu_+ \mu_- B_o^2} \left[\frac{\mu_o nk(T_+ + T_-)}{B_o} \right] \tag{8}$$

In the limit of no interaction between particles and no boundary effects we might expect the reduction in the magnetic field to be given by

$$\delta B = -\mu_o M \tag{9}$$

in which M, the magnetic dipole moment per unit volume, is given (2) by

$$\mu_o M = \mu_o nk(T_+ + T_-)/B_o \tag{10}$$

We see that Eq. 8 reduces to Eq. 10 when $\mu_+ \mu_-$ approaches infinity. In the limit of high collision rate the diamagnetic effect disappears as $\mu_+ \mu_-$ approaches zero. For large B, the magnetic field inhibits the radial diffusion so drastically that the diamagnetic effect also disappears. Ideally, the optimum diamagnetic effect is attainable with low-pressure, high-temperature, high-density plasmas and at values of the magnetic field that are consistent with $\mu_+ \mu_- B^2 = 1$. For our present purpose, the density of electrons must be low enough so that the density determined by the diamagnetic effect can also be determined by other means. Moreover, the measurement of diamagnetism in conjunction with a density-sensitive method, such as the microwave method, may offer a means of determining electron temperature.

Experiment

Two possible methods of detecting the diamagnetic effect are: (a) to measure the change in the magnetic field from a condition of no plasma to a plasma of density n and temperature T; (b) to take advantage of the fact that the susceptibility of the steady-state plasma is a function of the magnetic field. The first method is well suited to rapidly changing plasmas. For example, Eq. 8 indicates that the maximum change in the magnetic field occurs when $\mu_+ \mu_- B^2 = 1$. In a hydrogen discharge in which the ions are close to room temperature and the electrons are energetic, $\mu_+ p / \mu_- p = 1.4/29.3$, and we require $\mu_- B = 4.6 = eB/m\nu_c$. If we take $\nu_c = 6 \times 10^9 p$, we have B = 157p gauss (with p in mm Hg). At a pressure of 10 mm Hg, a field of approximately 1500 gauss is required. A flash tube can easily produce a density of 10^{14}/cc at a temperature of 3×10^4°K. For this case, $\delta B \approx 1.5$ gauss. The density can build up in a few microseconds. A coil of 10 turns with a cross-section area of approximately 1 cm^2 is expected to have an induced emf of approximately 0.10 volt. At lower pressures, and at correspondingly lower magnetic fields, the effect would be greater. However, the density cannot build up so rapidly at lower pressures, hence the pressure cannot be greatly decreased before the effect becomes smaller again.

The second method is more appropriate for steady-state plasmas. It is illustrated by the following example. The permeability μ of the plasma can be written

$$\frac{\mu - \mu_o}{\mu_o} = \frac{-\mu_+\mu_- \mu_o nk(T_+ + T_-)}{1 + \mu_-\mu_+ B^2} \tag{11}$$

in which B is the field that exists without the plasma. If we apply a field $B = B_o + B_1 \sin \omega t$, $B_1 \ll B_o$, we obtain, for the permeability,

$$\frac{\mu - \mu_o}{\mu_o} = - \frac{\mu_+\mu_-}{1 + \mu_+\mu_- B_o^2} \left(1 - \frac{2\mu_+\mu_- B_o B_1}{1 + \mu_+\mu_- B_o^2} \sin \omega t \right) \mu_o nk(T_+ + T_-) \tag{12}$$

It can be shown that the signal introduced by the plasma is

$$V = NA\,\omega B_1 \cos \omega t \left[\frac{\mu_+\mu_- \left(1 - \mu_+\mu_- B_o^2\right)}{1 + \mu_+\mu_- B_o^2} \right] \mu_o nk(T_+ + T_-) \tag{13}$$

By suitable amplification, the ac signal can be observed. We plan to use both experimental methods; preliminary results indicate that the effect exists.

E. I. Gordon

References

1. M. Steenbeck, Über die magnetischen Eigenschaften des Plasmas von Gasentladungen, Wiss. Veröff. Siemens-Werken 15, 2, 1 (1936).
2. H. Alfvén, Cosmical Electrodynamics (Clarendon Press, Oxford, 1950).
3. W. P. Allis, Motions of ions and electrons, Handbuch der Physik, Vol. 21, 1956; Technical Report 299, Research Laboratory of Electronics, M.I.T., June 13, 1956.

F. INHOMOGENEOUS MAGNETIC-FIELD DESIGN

1. Introduction

Study of the physics of ionized gases has created a need for synthesizing inhomogeneous magnetic fields with a high degree of accuracy. This problem was considered by L. J. Chu, who suggested a synthesis procedure based on the technique of establishing an analytic expression for the desired magnetic-field solution in a specified region of space. He suggested that the desired fields be generated by current-carrying conductors and magnetic boundaries located outside the region with which we were concerned, and that the magnitude and distribution of the current be determined by using the relation that, at the surface of an infinitely thin current sheet of current density

$\bar{J}$, $\bar{n} \times \bar{H} = \bar{J}$, where $\bar{n}$ is the outward-directed normal of the surface, and $\bar{H}$ is the magnetic-field intensity. He pointed out that current sheets located along lines of equal flux, and magnetic material located along lines of equal potential would provide perfect terminating boundaries for the magnetic-field solution.

The accuracy with which the magnetic field can be synthesized by Chu's method depends upon the degree to which the terminating boundaries approximate the assumed boundary conditions. The major synthesis problem is, then, to determine how well the current density J that is produced in finite conductors approximates the current sheets of zero thickness. We could use a current that is distributed over a finite region of space by matching solutions of the Laplace and Poisson equations along specified boundaries. This approach is difficult analytically and will not be discussed.

The design of a low-power magnet, which used the Chu procedure, was carried out by R. G. Meyerand, Jr. His experimental results indicated that a small finite distribution of current did not greatly affect the fields calculated with idealized sources. On the basis of these positive results, a new design of a higher power magnet was undertaken, which will now be discussed.

2. Specifications

Synthesize a magnetic field that is an axially symmetric 1000-gauss field with a uniformity of not less than 0.5 per cent over a center region of 6-cm length and 1-cm radius, with a ratio of maximum to minimum field intensity along the axis of 5 or higher. Design the magnet for continuous operation. Use one of the following power sources: 20-kw, 220-volt thyratron-controlled rectifier; 300-amp, 26-volt dc generator; or 3000-amp, 12-volt dc generator. Provide four 0.5-inch holes spaced symmetrically around the center of the magnet for instrumenting the region of uniform field.

3. Analytic Expression for the Magnetic Field

The magnetic field is in free space, and consequently it must satisfy the Laplace equation, $\nabla^2\psi = 0$, in this region. Since the field is axially symmetric, cylindrical coordinates are the logical choice, and, because of the symmetry in the ϕ-direction, the scalar potential must satisfy the equation

$$\nabla^2\psi(r, z) = \frac{1}{r}\frac{\partial}{\partial r}\left(\tau \frac{\partial \psi}{\partial r}\right) + \frac{\partial^2 \psi}{\partial z^2} = 0$$

General solutions of this equation take the well-known form

$$\psi = \sum_{n=1}^{\infty} \left[A_n J_o(k_n r) + B_n N_o(k_n r)\right]\left[C_n e^{k_n z} + D_n e^{-k_n z}\right]$$

The terms in $N_o(k_n r)$ can be discarded, since ψ and $\overline{B}$ must be finite at $r = 0$. The magnetic-field solutions corresponding to ψ are calculated as $\overline{B} = -\overline{\nabla}\psi$. For $\overline{B}$ finite at $r = 0$, they take the form

$$\overline{B} = -\bar{a}_r \frac{\partial \psi}{\partial r} - \bar{a}_z \frac{\partial \psi}{\partial z} = \bar{a}_r B_r + \bar{a}_z B_z = \sum_{n=1}^{\infty} \left\{ + \bar{a}_r A_n k_n J_1(k_n r) \left[C_n e^{k_n z} + D_n e^{-k_n z} \right] \right.$$

$$\left. - \bar{a}_z A_n J_o(k_n r) \left[C_n k_n e^{k_n z} - D_n k_n e^{-k_n z} \right] \right\}$$

The B_z component of the magnetic field must increase for z that is appreciably removed from $z = 0$, and it must be symmetrical about the point $z = 0$; hence B_z must be an even function of z. This condition can be met for both real and imaginary values of k. Consequently, allowed solutions of ψ and $\overline{B}$ take the general form:

$$\psi = \sum_{n=1}^{\infty} \left[A'_n J_o(k_n r) \sinh (k_n z) + B'_n I_o(k_n r) \sin (k_n z) \right]$$

$$\overline{B} = \sum_{n=1}^{\infty} \left\{ \bar{a}_r \left[A'_n k_n J_1(k_n r) \sinh k_n z - B'_n k_n I_1(k_n r) \sin k_n z \right] \right.$$

$$\left. - \bar{a}_z \left[A'_n k_n J_o(k_n r) \cosh k_n z + B'_n k_n I_o(k_n r) \cos k_n z \right] \right\}$$

In the field solution which these general solutions must satisfy B_z is very uniform over a region of space around $r = 0$, $z = 0$, and increases rapidly for z that is outside this uniform region. One way to obtain this result is to define the desired field distribution, make a Fourier expansion of the field along the z-axis, and match coefficients with the general expression. However, a much simpler field solution that meets the desired conditions can be obtained by observing the variation of B_r and B_z along the z-axis ($r = 0$) and along a radius at $z = 0$ for small values of z and r. Thus the four following relations characterize the variations of B for small r and z:

$$\left. \begin{aligned} &\sum_{n=1}^{\infty} A'_n \sinh k_n z - B'_n \sin k_n z \\ &\sum_{n=1}^{\infty} A'_n \cosh k_n z + B'_n \cos k_n z \end{aligned} \right\} \quad \text{for } r = 0$$

$$\left.\begin{aligned}&\sum_{n=1}^{\infty} A_n' J_1(k_n r) - B_n' I_1(k_n r)\\ &\sum_{n=1}^{\infty} A_n' J_o(k_n r) + B_n' I_o(k_n r)\end{aligned}\right\} \quad \text{for } z \approx 0$$

From a power-series expansion of the eight functions sinh kz, sin kz, cosh kz, cos kz, $J_1(kr)$, $I_1(kr)$, $J_o(kr)$, and $I_o(kr)$, it follows that if $A_n = B_n$ and $k_n = k$, the variations in B_r and B_z around r = 0 and z = 0 become

$$\left.\begin{aligned}\sinh kz - \sin kz &= \frac{2(kz)^3}{3!} + \frac{2(kz)^7}{7!} \cdots\\ \cosh kz + \cos kz &= 2 + \frac{2(kz)^4}{4!} + \frac{2(kz)^8}{8!} \cdots\end{aligned}\right\} \quad \begin{aligned}&\text{for} \quad r = 0\\ &A_n = B_n\\ &k_n = k\end{aligned}$$

$$\left.\begin{aligned}J_1(kr) - I_1(kr) &= -\frac{2(kr/2)^3}{1!2!} - \frac{2(kr/2)^7}{3!4!}\\ J_o(kr) + I_o(kr) &= 2 + \frac{2(kr/2)^4}{2!2!} + \frac{2(kr/2)^8}{4!4!}\end{aligned}\right\} \quad \begin{aligned}&\text{for} \quad z \approx 0\\ &A_n = B_n\\ &k_n = k\end{aligned}$$

These equations show that if only two terms in the power-series expansion for the magnetic field are kept, the first important term in the variation of the B_z component along the z-axis is $(kz)^4/4!$. Along a radius at z = 0 it is $(kr)^4/2!2!$. Clearly, then, for small z and r, a uniform magnetic field can be obtained by using the simple scalar field

$$\psi = A[J_o(kr) \sinh (kz) + I_o(kr) \sin (kz)]$$

which gives a magnetic field

$$\overline{B} = Ak\left\{\bar{a}_r[J_1(kr) \sinh (kz) - I_1(kr) \sin (kz)] - \bar{a}_z[J_o(kr) \cosh (kz) + I_o(kr) \cos (kz)]\right\}$$

This particular expression for the magnetic field has the advantage of analytic simplicity, excellent uniformity of B_z around z = 0, r = 0, and a very rapid increase in B_z for large z. Thus a magnet can be designed for good uniformity over a central region

and a large ratio of B_{max} to B_{min} without being excessively long.

4. Evaluation of the Magnet's Boundary Condition

Choice of the principal dimension of the magnet is somewhat arbitrary, since many configurations will meet the specifications. The main problem in a large magnet is the total power consumed, and this power is reduced (within limits) by minimizing the dimensions. The dimensions chosen were, approximately, an 8-cm radius and a 60-cm length for a B_{max} to B_{min} ratio of 5. This gave a B_z uniform within 0.5 per cent over a region of approximately 11 cm along the z-axis and of 6-cm radius at z = 0. Since this uniform-field region was twice the desired size, a smaller magnet could have been designed. After considering possible difficulties in construction and the effects of finite current distribution, the factor of 2 in the size of the region at uniform B was kept.

The desired magnetic-field strength at the center of the magnet is 1000 gauss (0.1 weber/m^2), and a ratio of B_{max} to B_{min} of at least 5 along the axis at 30 cm from the center is desired. The field solutions that satisfy these conditions are:

$$\psi = \frac{-0.05}{k}\left\{I_o(kr)\sin(kz) + J_o(kr)\sinh(kz)\right\}$$

$$\bar{B} = -\bar{\nabla}\psi = 0.05\left\{\bar{a}_r[I_1(kr)\sin(kz) - J_1(kr)\sinh(kz)] + \bar{a}_z[I_o(kr)\cos(kz) + J_o(kr)\cosh(kz)]\right\}$$

where $k = \pi/0.3$, and r and z are in meters.

With the $\bar{B}$ field determined, the boundary condition can be established. A current distribution that will produce this field can be evaluated by finding the magnetic-field intensity along constant-flux contours of the scalar flux field Φ. The constant-flux contours are determined by recognizing that the constant-potential contours of ψ and constant-flux contours of Φ are orthogonal. These two orthogonal fields must also satisfy the condition that their gradients are orthogonal; that is, $\nabla\psi \cdot \nabla\Phi = 0$. One simple way to find the scalar flux field Φ is to recognize that it is the measure of the flux that passes a cylindrical surface normal to the z-axis. Thus

$$\Phi = \int_0^r \bar{B} \cdot d\bar{a} = \int_0^r B_z\, 2\pi r\, dr$$

For the value of B chosen, the scalar flux field becomes simply

$$\Phi = 0.03\left\{rI_1(kr)\cos(kz) + rJ_1(kr)\cosh(kz)\right\}$$

This scalar flux field can be shown to satisfy the orthogonality condition $\nabla\psi \cdot \nabla\Phi = 0$.

The surface contour of the magnet was determined by a line of constant Φ, and the constant-flux surface that intersects the point z = 0, r = 0.08 meter was chosen. This gives a flux surface of $\Phi = 0.0020158$ weber or 201,580 lines. The data for the practical magnet design were determined by finding the contour for $\Phi = \Phi_s = 0.0020158$ and the magnetic-field intensity

$$H_z\Big|_{\Phi_s} = \frac{B_3}{\mu_o}\Big|_{\Phi_s}$$

evaluated along the constant-flux contour Φ_s. These data are plotted in Fig. II-7.

5. Design

The calculations illustrated in Fig. II-7 show that, at z = 0, a current of 8000 amp/meter length is required. At z = 0.30 meter, the required current is 36,000 amp/meter length, which gives a B_{max}/B_{min} ratio of 5.3 on the z-axis. At z = 0.35 meter, the required current is 64,500 amp/meter length, which produces a B_{max}/B_{min} ratio of 9.3 on the z-axis. These currents are obviously very large and hence, if the conventional figures of 150,000 to 300,000 amp/meter^2 were used, copper thicknesses as large as 0.5 meter would be required at the end of the magnet. Any such thickness is impossible on simple physical grounds. Moreover, the current densities were calculated with the assumption that the current sheets are infinitely thin,

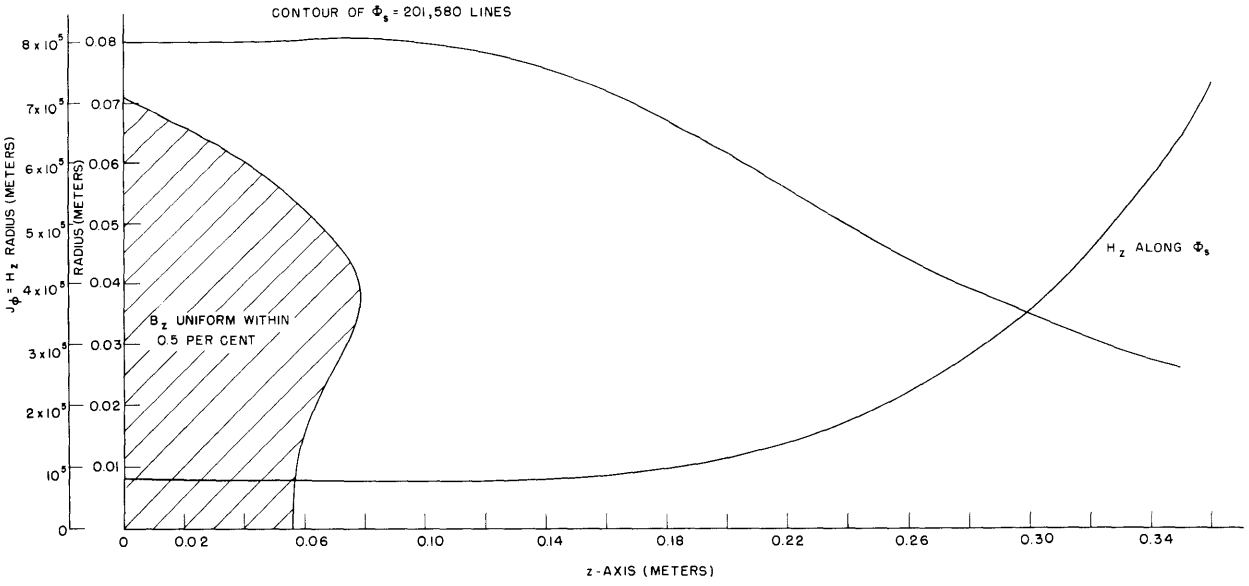

Fig. II-7. Constant-flux contour and axial current density.

and any thickness of copper that distributes the current over a region of the same order of magnitude as the major dimension of the magnet would not approximate the calculated field solution.

The amount of copper needed to carry the current is determined primarily by considering the heat dissipated in I^2R in the windings. The elimination of heat from the windings is essentially a problem in heat transfer across the insulation around the copper wires to an exterior surface which dissipates the heat by radiation, convection, and conduction. The problem of heat transfer can be simplified by keeping the thickness of the insulating boundaries between heat source and heat sink minimum. This problem was best solved by using a single-layer magnet energized from a high-current, low-voltage source. The single-layer design has only one 0.001-inch insulating barrier between the heat source and the heat sink. An average heat conductivity of insulating materials is 0.001 watt-cm/°C; therefore, across a 1-cm^2 surface that is 1 mil thick (0.00254 cm), a thermal power transfer of 0.4 watt/°C can be obtained. This heat-transfer figure is very attractive and indicates that a single-layer magnet with very high current densities would not exceed 100°C to 150°C rise in the hottest parts. This has still to be checked experimentally.

The design of a single-layer winding to produce a continuously varying current along the axis of the magnet presented some difficulty. The simplest solution was found by varying the width of each turn along the axis of the magnet so that a constant value of total current approximated the desired current distribution. Calculations on the basis of a 2000-amp source led to conductor sizes of 1 inch maximum width in the center of the magnet to 0.1 inch minimum width at the end of the magnet. These dimensions were reasonable, and, since a 3000-amp, 12-volt generator was available, a figure of 2000 amp to produce 1000 gauss at the center of the magnet was chosen. The width of successive turns was calculated from the curve for H_z shown in Fig. II-7 by the relation

$$I = 2000 = \int_{z_1}^{z_2} |H_z| \, dz$$

The widths for each turn obtained from these calculations are included in Table II-1.

Taking into account the maximum power available from the generator, the heat transfer across a surface of approximately 0.4 watt/cm^2/°C, and the copper thickness that would reasonably approximate a very thin current sheet, we chose a copper thickness of 0.35 inch over the length from z = 0 to z = 30 cm, which gave a B_{max}/B_{min} ratio of 5.3. The section of the magnet between z = 30 cm and z = 35 cm was designed with a copper thickness of 0.5 inch, since this section was far enough from the center where the uniform field is desired so that the additional thickness would not be

Table II-1. Copper Winding – Dimension of Each Turn.

Turn No.	z(meters)	r(meters)
0	0	0.080
1	0.02502	0.080
2	0.05028	0.080
3	0.07600	0.080
4	0.10208	0.080
5	0.12792	0.07771
6	0.15228	0.07384
7	0.17399	0.06884
8	0.19263	0.06371
9	0.20846	0.05906
10	0.22201	0.05504
11	0.23374	0.05163
12	0.24406	0.04872
13	0.25325	0.04622
14	0.26152	0.04405
15	0.26903	0.04216
16	0.27592	0.04050
17	0.28228	0.03902
18	0.28818	0.03769
19	0.29369	0.03650
20	0.29886	0.03540
21	0.30372	0.03442
22	0.30832	0.03350
23	0.31268	0.03267
24	0.31683	0.03189
25	0.32079	0.03116
26	0.32456	0.03050
27	0.32817	0.02986
28	0.33164	0.02927
29	0.33497	0.02872
30	0.33818	0.02819
31	0.34128	0.02769
32	0.34426	0.02723
33	0.34715	0.02679
34	0.34995	0.02636

detrimental. This increased thickness appreciably reduced the dissipated power. The section from 30 cm to 35 cm was designed as a removable section, so that the magnet can be operated with a B_{max}/B_{min} ratio of 5.3 or a B_{max}/B_{min} ratio of 9.3.

The outside surface of the current sheet is an equal-potential line which was simulated by an iron boundary. Iron boundaries were placed across both ends of the magnet on equal-potential lines. The total flux enclosed by the magnet is approximately 200,000 lines for 1000 gauss in the center. To prevent saturation, the magnet was designed with a 0.25-inch iron shell from z = 0 to z = 30, and a 0.5-inch shell from z = 30 to z = 35, with end caps 1 inch thick.

The copper windings were fastened to the iron shell by a thin layer of insulating varnish (not more than 1 mil thick) that holds the copper winding and iron shell together as one structural unit. The heat is conducted from the copper across the insulation to the iron; water-carrying conductors on the surface of the iron take the heat away. The total power dissipated is 10.5 kw for a B_{max}/B_{min} ratio of 5.3, or 18.5 kw for a B_{max}/B_{min} ratio of 9.3. The maximum water flow for a 50°C rise would be approximately 1.5 gallons/minute. See Fig. II-8.

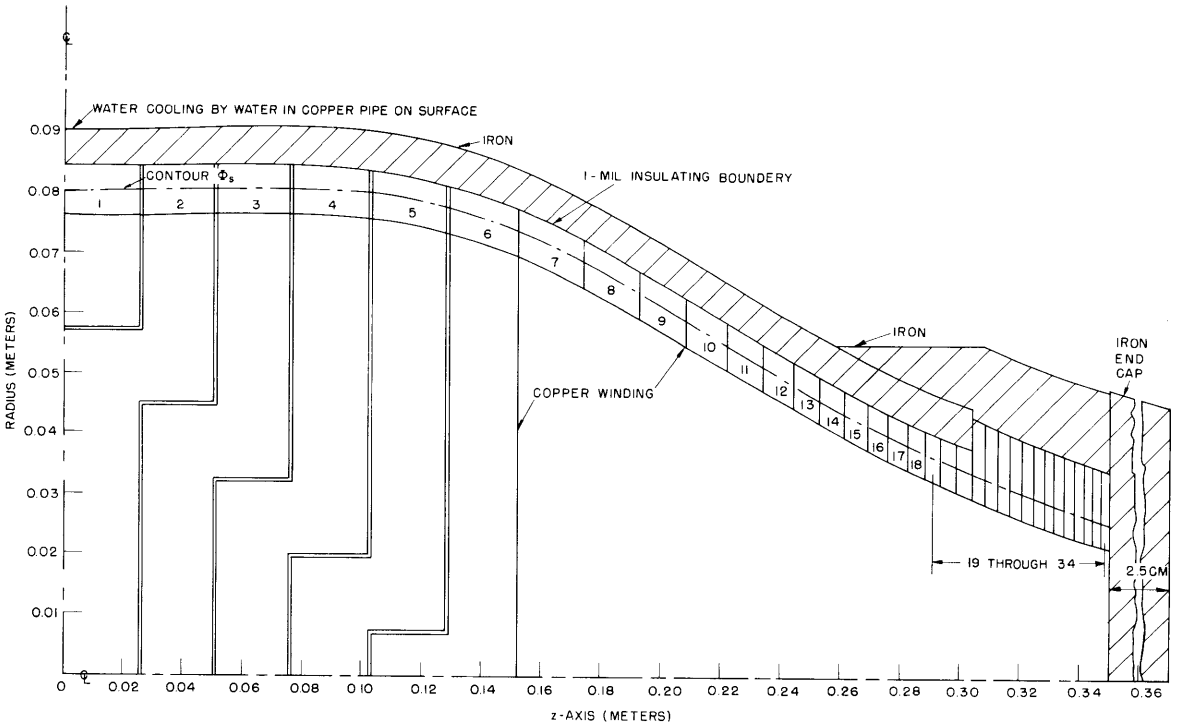

Fig. II-8. Cross section of magnet with copper winding and iron shell.

6. Construction

The general construction of the magnet is quite simple, with the exception of the single-layer winding. The winding was constructed by building a form of hardwood covered with wax. The turns were placed along the axis of the form, with small insulating spaces 10 mils thick. The winding was electroplated on the form. This produced a stress-free winding with the insulation already in place between the turns. The winding was machined on the outer surface to match the iron boundary and fastened to the iron with insulating varnish. The winding and iron boundary forms a single structural unit.

The magnet is being constructed; final details will be reported later.

D. C. White